Multidimensional Beam Coverage Millimeter-Wave Phased Antenna Array

Zhonghe Zhang, Jiupei Shi, Sai-Wai Wong*,Yejun He
State Key Laboratory of Radio Frequency Heterogeneous Integration
Sino-British Antennas and Propagation Joint Labortory, Ministry of Science and Technology of China
Guangdong Engineering Research Center of Base Station Antennas and Propagation
Shenzhen Key Laboratory of Antennas and Propagation
College of Electronics and Information Engineering, Shenzhen University, 518060, China
Email: 2150432016@email.szu.edu.cn，2250432008@email.szu.edu.cn，wongsaiwai@ieee.org，heyejun@126.com

2024 IEEE International Workshop on Radio Frequency and Antenna Technologies (iWRF&AT) | 979-8-3503-8476-5/24/$31.00 ©2024 IEEE | DOI: 10.1109/iWRFAT61200.2024.10594629

***Abstract*—This article introduces a millimeter wave patch dipole antenna array. It examines and addresses coupling effects by simultaneously exciting common mode (CM) and differential mode (DM) signals on two dipoles separated by 1/4 λ_0. Manipulating the phase difference between two dipole antennas results in four entirely different radiation patterns: omnidirectional, two distinct unidirectional patterns, and a bidirectional radiation pattern. Encompassing a 360° beam coverage, these four radiation patterns serve as a solution for multi-dimensional communication within millimeter wave applications.**

***Index Terms*—Millimeter wave antenna array, 360° beam coverage, common mode (CM) and difference mode (DM).**

I. Introduction

The 5G wireless system boasts several advantages such as high-speed data transfer, low latency, large capacity, high-density connectivity, and the advantages of millimeter-wave communication. With data transfer rates reaching several Gb/s and reduced communication latency supporting real time applications, it meets the growing demands for increased connectivity through its large capacity and high-density connections. Additionally, the broadband advantages of millimeter wave [1] communication further enhance the possibilities for high-speed data transfer.

A singular beam coverage struggles to meet the growingly intricate communication needs. To address this, a multi-polarized antenna array [2] has been proposed. The multi-mode patch elements can offer wideband coverage (TM_{01} or TM_{10} modes) alongside a singular mode (TM_{21} mode). The achievement of high isolation dual-polarized antennas in [3] is attained through the implementation of feed structures within diverse metallic cavities. Adjusting the length of metal pillars within metallic cavities achieves frequency-reconfigurable antennas to accommodate diverse communication needs [4]. However, these antennas are limited to achieving single-directional beam coverage. The current trend aims to achieve multidimensional beam coverage.

In [5], three sets of patch antennas were deployed on a mobile phone, covering three different directions. An improvement outlined in [6] involved integrating end-fire and broadside antennas within the same cavity, reducing overall volume. In [7], a dual-port antenna was utilized to achieve beam coverage in different directions by adjusting the phase between the two ports. In [8], a vertically polarized 360° azimuth scanning phased array based on wide-beamwidth elements was proposed. The array consists of two back-to-back monopole antenna arrays. In [9]-[10], a universal decoupling technique based on the elimination of common mode (CM) and differential mode (DM) is introduced.

In this paper, the coupling issue between two dipole antennas positioned a quarter wavelength apart is addressed through common mode-differential mode cancellation. Multiple beam coverage is achieved by adjusting the phase difference between ports. The array design and the beam coverage under various phase difference modes are discussed.

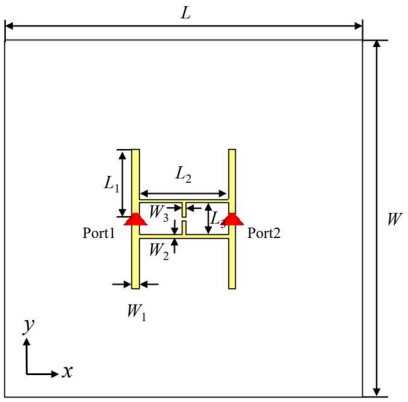

Fig. 1. Model of two extremely closely spaced dipole with a side-by-side distance 1/4 λ_0. L=10, W=10, L_1=1.83, W_1=0.2, L_2=2.5, W_2=0.1, L_3=0.4. W_3=0.1, (unit: mm).

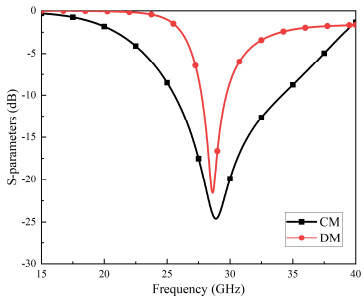

Fig. 2. Return loss of common mode and differential mode

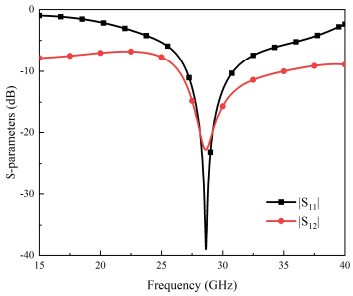

Fig. 3. Return loss of two dipole antenna.

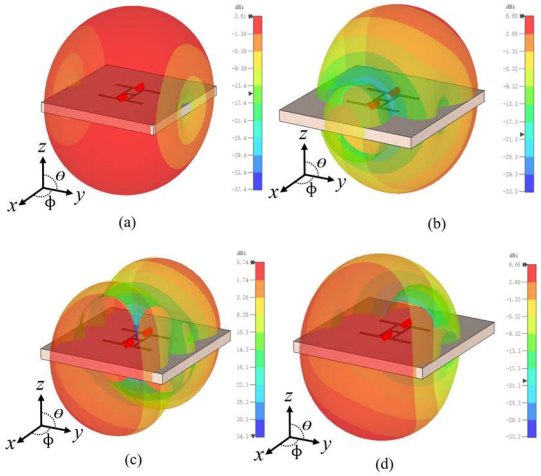

Fig. 4. Simulated 3D radiation pattern. (a) 0° phase difference. (b) 90° phase difference. (c) 180° phase difference. (d) 270° phase difference.

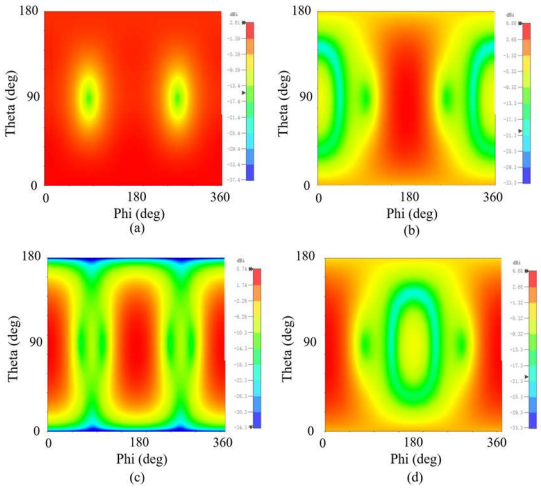

Fig. 5. Simulated 2D contour radiation pattern. (a) 0° phase difference. (b) 90° phase difference. (c) 180° phase difference. (d) 270° phase difference.

II. Design of FSA and Antenna

Modeling of two closely spaced dipoles with a side-by-side distance of 1/4 λ_0 is designed, as shown in Fig. 1, on a 0.787 thick Rogers 5880 substrate. The antenna consists of two equally sized patch dipoles, each fed by its own lumped port. Between the two dipole antennas, there is a horizontal branch of length L_2, with a vertical branch of length L_3 connected below it. This differs from [9] in that

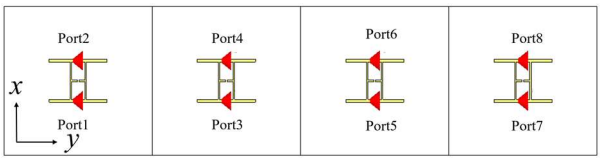

Fig. 6. 2×4 phased antenna array with 8 ports.

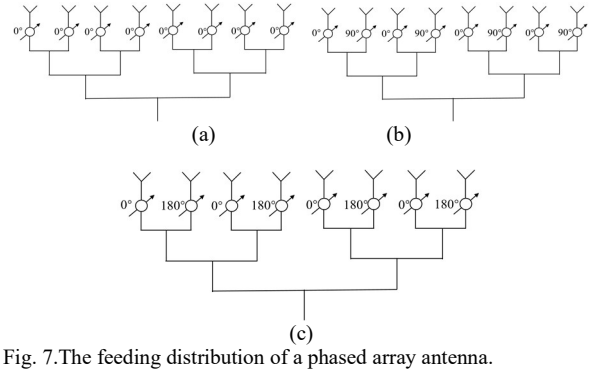

Fig. 7.The feeding distribution of a phased array antenna.

the equivalent capacitance across the gap between the two branches replaces the capacitor, providing an effective simplification in antenna design. The common mode and differential mode return losses of the antenna through the connection of the two branches are illustrated in Fig. 2, operating at the same frequency and staying below -10 dB. The calculation for common mode and differential mode return losses is represented by (1) and (2) demonstrating effective decoupling between the two antennas when resonating at identical frequencies. When $S_{DM} = S_{CM}$, $S_{21} = 0$. The simulated antenna's S-parameter return loss is shown in Fig. 3, where S_{11} is below -38 dB and S_{21} is below -22 dB.

$$S_{CM} = (S_{11} + S_{12} + S_{21} + S_{22})/2 \quad (1)$$

$$S_{DM} = (S_{11} - S_{12} - S_{21} + S_{22})/2 \quad (2)$$

Changing the phase discrepancy between the two dipole patch antennas can produce diverse radiation patterns. The Simulated 3D radiation pattern at different phase differences is shown in Fig. 4. When the phase difference is 0°, both antennas maintain common-mode radiation, and the antennas maintain omnidirectional coverage on the xoz plane, as shown in Fig. 4(a). When the phase difference is 90°, the electromagnetic waves in the +x direction cancel each other out due to the opposite phase and the same amplitude, while in the -x direction, the waves add up due to the same phase and amplitude, resulting in the directional beam in the -x direction as shown in Fig. 4(b). When the phase difference is 180°, the antenna exhibits differential mode radiation. The electromagnetic waves cancel each other out in the Z direction, forming a radiation null. Meanwhile, they add up in the x direction, resulting in the dual-beam antenna as shown in Fig. 4(c). When the phase difference is 270°, the electromagnetic waves exhibit opposite phases in the -x direction, canceling each other out, while having the same phase and amplitude in

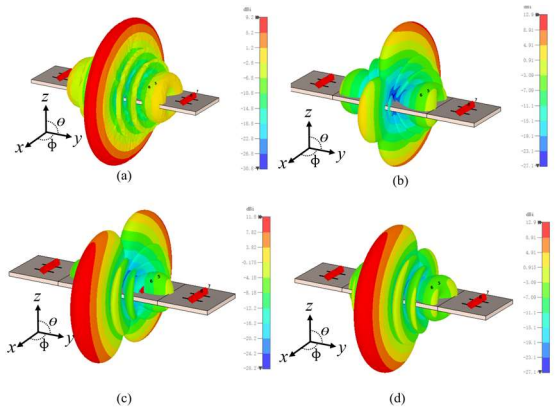

Fig. 8. Simulated 3D radiation pattern. (a) 0° phase difference. (b) 90° phase difference. (c) 180° phase difference. (d) 270° phase difference.

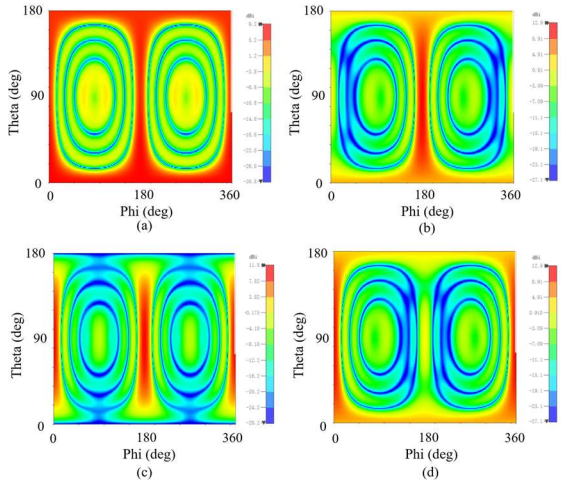

Fig. 9. Simulated 2D contour radiation pattern. (a) 0° phase difference. (b) 90° phase difference. (c) 180° phase difference. (d) 270° phase difference.

the +x direction, thereby adding up and producing radiation in the +x direction as depicted in Fig .4(d).

The simulated 2D contour radiation pattern, as shown in Fig. 5, demonstrates complete 360° radiation coverage across the xoz plane. Various phase distributions enable diverse millimeter-wave communication requirements.

III. Design of Antenna Array

Millimeter waves operate at higher frequencies with broader bandwidths but limited propagation distances. High-gain antennas can offer extended coverage and enhance data reliability. Phased array antennas are commonly used to achieve high gain. As explained earlier, antennas have a natural radiation null in the y-axis. Therefore, a millimeter-wave antenna array arranged along the y-axis has been designed, depicted in Fig. 6.

Different phase differences between ports can achieve different high-gain radiation beams in antennas. The antenna feeding and phase distributions are depicted in Fig. 7. Dipole antennas parallel to the x-axis can adjust the phase differences. Fig. 7(a) represents common mode feeding, Fig. 7(b) shows a 90° phase difference, and Fig. 7(c) demonstrates differential mode feeding, where the phase difference of 270° is similar to 90° but with the beam direction reversed.

The 3D radiation pattern and 2D contour radiation pattern of the array are depicted in Fig. 8 and Fig. 9. The gains for the four distinct radiation patterns are 9.2 dBi, 12.9 dBi, 11.8 dBi, and 12.9 dBi, enabling high-gain beam scanning on the xoz plane

IV. Conclusion

In this work, a coupled 1/4 λ_0 dipole patch antenna is utilized, achieving low mutual coupling below -22dB under ideal conditions. Maintaining the equal amplitude between two antennas, four different radiation modes are realized by altering the phase,enabling 360° beam coverage on the xoz plane and forming an array. This design exhibits advantages such as low profile, cost-effectiveness, and multi-mode multi-dimensional beam coverage.

Acknowledgement

This work is supported by National Natural Science Foundation of China under grant 62171289.

References

[1] J. Guo, Y. Hu, and W. Hong, "A 45° polarized wideband and wide-coverage patch antenna array for millimeter-wave communication," *IEEE Tran. Antennas Propag.*, vol. 70, no. 3, pp. 1919-1930, Mar. 2021.

[2] G. F. Gao, X. Ding, Y. F. Cheng, and W. Shao, "Dual-polarized wide-angle scanning phased array based on multimode patch elements," *IEEE Antennas Wireless Propag. Lett.,* vol. 18, no. 3, pp. 546-550, Mar. 2019.

[3] R. S. Chen, L. Zhu, J. Y. Lin, S. W. Wong, Y. Yang, Y. Li, L. Zhang, and Y. He, "High-isolation in-band full-duplex cavity-backed slot antennas in a single resonant cavity," *IEEE Trans. Antennas Propag.*, vol. 69, no. 11, pp. 7092-7102, Nov. 2020.

[4] R. S. Chen, L. Zhu, S. W. Wong, X. Z. Yu, Y. Li, W. He, L. Zhang, and Y. He., "Novel reconfigurable full-metal cavity-backed slot antennas using movable metal posts," *IEEE Trans. Antennas Propag.*, vol. 69, no. 10, pp. 6154-6164, Oct. 2021.

[5] N. Ojaroudiparchin, M. Shen, S. Zhang, and G. F. Pedersen, "A switchable 3-D-coverage-phased array antenna package for 5G mobile terminals," *IEEE Antennas Wireless Propag. Lett.*, vol. 15, pp. 1747-1750, 2016.

[6] B. Kim, M. Kim, D. Lee, J. Lee, Y. Youn, and W. Hong, "A Shared-Aperture Cavity Slot Antenna-in-Package Concept Featuring End-Fire and Broadside Radiation for Enhanced Beam Coverage of mmWave Mobile Devices," *IEEE Trans. Antennas Propag.*, vol. 71, no. 2, pp. 1378-1390, Feb. 2023.

[7] J. Zhang, J. Geng, H. Zhou, C. Ren, K. Wang, S. Yang, et al., "Dual-port phase antenna and its application in 1-D arrays to 2-D scanning," *IEEE Trans. Antennas Propag.*, vol. 69, no. 11, pp. 7508-7520, Nov. 2021.

[8] J. Hu, Y. Li, and Z. Zhang, "Vertically Polarized 360° Azimuth Scanning Array," *IEEE Antennas Wireless Propag. Lett.,* vol. 21, no. 5, pp. 898-902, May 2022.

[9] L. Sun, Y. Li, Z. Zhang, and H. Wang, "Antenna decoupling by common and differential modes cancellation," *IEEE Trans. Antennas Propag.*, vol. 69, no. 2, pp. 672-682, Feb. 2020.

[10] L. Sun, Y. Li, Z. Zhang, and H. Wang, "Self-decoupled MIMO antenna pair with shared radiator for 5G smartphones," *IEEE Trans. Antennas and Propag.*, vol. 68, no. 5, pp. 3423-3432, May 2020.